JOURNAL OF MATERIALS SCIENCE MATERIALS IN MEDICINE 5 (1994) 457–462

Stability of hydroxylapatite plasma-sprayed coated Ti–6Al–4V under cyclic bending in simulated physiological solutions

R. L. REIS, F. J. MONTEIRO
INEB-National Institute for Biomedical Engineering, Faculty of Engineering, University of Porto, Rua dos Bragas-4099 PORTO Codex, Portugal

G. W. HASTINGS
I.R.C in Biomedical Materials, Queen Mary & Westfield College, University of London, Mile End Road, E1 4NS, London, UK

The aim of this research was to study the stability of plasma-sprayed coated metal systems and to evaluate their susceptibility to the occurrence of corrosion fatigue. Hydroxylapatite plasma-sprayed coated samples of Ti–6Al–4V were studied under cyclic bending. During fatigue testing samples were immersed in a simulated physiological solution and mechanical and electrochemical degradation were monitored. Applied loads were intended to crack the ceramic coating and not the metal substrate. Electrochemical impedance spectroscopy was used to further characterize the electrochemical behaviour. No increase in tendency to corrode was detected in open-circuit corrosion fatigue testing. It appears as if the coating cracking does not increase metal substrate corrosion susceptibility. The coating integrity has been seriously affected, with marked decrease in thickness, due to the synergistic effect of load and presence of simulated body fluids environment. Impedance results, however, show a general tendency to an increase in corrosion kinetics after corrosion fatigue testing.

1. Introduction

Hydroxylapatite (HA) coatings are porous to permit bone ingrowth [1, 2] and attachment [2, 3]. However, HA coatings may easily crack under load [4], and the eventual effect of such fracture on metal substrate passive behaviour might induce some danger if these materials are used as implants. Combination of cyclic loading, in service conditions, and aggressive species present in the body fluids [5], could cause a synergistic effect. The aim of this work was to simulate these conditions and assess the stability of HA-coated Ti–6Al–4V.

The clinical application of bioactive hydroxylapatite coated implants is attracting considerable interest, with emphasis on the use of plasma-sprayed coatings to combine the superior mechanical performance of the metal component with the excellent biological responses of HA [6]. Some authors [6, 7] claim that HA should act as a biological barrier to reduce toxic responses caused by the release of metallic ions from metal substrate into the bone. Some doubts remain as to what might be the long-term stability of the coating [8]. Studies on the behaviour of metal substrate under cyclic loading may be found in the literature [9–12]. In all the listed references, high loads have been applied, with the intention of causing fracture and set typical S–N curves. In many cases, simulated physiological solutions were used [9, 10], but coated metal electrochemical behaviour is not highlighted. Fundamental studies of the stability of coating itself are rare [5, 8, 13], and have generally been performed under static load conditions [5, 13] or in dry conditions [14].

In this work a new approach to the characterization of coated metal systems is presented. The testing method has been described elsewhere [15]. Loads aim at cracking the ceramic without leading to substrate fatigue failure. Both electrochemical corrosion susceptibility and mechanical degradation levels are followed during test under real-time conditions. After testing, metal ion release levels, solution pH, coating thickness and microstructure, were analysed. To complete the electrochemical characterization, samples were tested using electrochemical impedance spectroscopy, both before and after corrosion fatigue testing. This technique is still unusual for biomaterials and coated systems interface characterization [16, 17].

2. Materials and methods

2.1. Materials

Ti–6Al–4V hydroxylapatite plasma-sprayed coated samples, beam shaped with $180 \times 30 \times 6$ mm, were tested. At this stage only 50 μm thick coatings (one side) were studied. All coatings were performed by Plasma Biotal Company, Tideswell, UK, using an atmospheric plasma-spraying unit and with the same

0957–4530

coating parameters as used for commercial coatings. Metal substrate was annealed at 750 °C, for 2 h, and air cooled. An α–β acicular microstructure was produced, presenting a yield strength of 865 MPa and an elongation of 16%. Then the substrate was alumina grit blasted to a surface roughness R_A (mean roughness, DIN 4762) = 1.66 μm and R_z (roughness depth, DIN 4768) = 5.61 μm and passivated in nitric acid (HNO_3) prior to coating.

2.2. Open-circuit corrosion fatigue experiments

An apparatus suitable for performing corrosion fatigue experiments on ceramic coated biomaterials was designed and built. The testing method used has already been fully described [15]. Fig. 1 shows the experimental set-up. All tests were performed in the following conditions: four-point bending loading (controlled deflection), sine wave, $R(\sigma_{min}/\sigma_{max}) = 0$, σ_{max} (for time = 0) = 80 MPa or 40 MPa, frequency = 10 Hz, testing length = 10^6 cycles. Tests were always carried out in deflection-imposed conditions and initial applied stress levels were chosen intending to crack the coating and not the metal substrate. Applied stress levels (for time = 0) were controlled by means of changing imposed deflection and loading span. Open-circuit corrosion potential was recorded with respect to the standard calomel electrode with changing time. Two different simulated physiological solutions: Hank's balanced salt solution (HBSS) and isotonic saline solution (0.15 M NaCl) (ISS) were used as testing environments. All tests were carried out at room temperature (20 ± 2 °C). pH of the initial and final solutions (after corrosion fatigue experiments) were measured. Solution was in contact with air and was agitated continuously due to the cyclic movement. Test were always performed in oxygen saturation conditions, at approximately 6 ppm of dissolved oxygen. Tests for fatigue behaviour were also carried out in air. Samples were supported by two load transducers (in a four-point bending scheme) and only the region between the inner rollers was in contact with the testing solution. The coated face was always facing the solution. Metal substrate uncoated sides were always isolated using Lacomit varnish. A data acquisition system and a software package, BIOFATCOR®, were developed and used to control all tests.

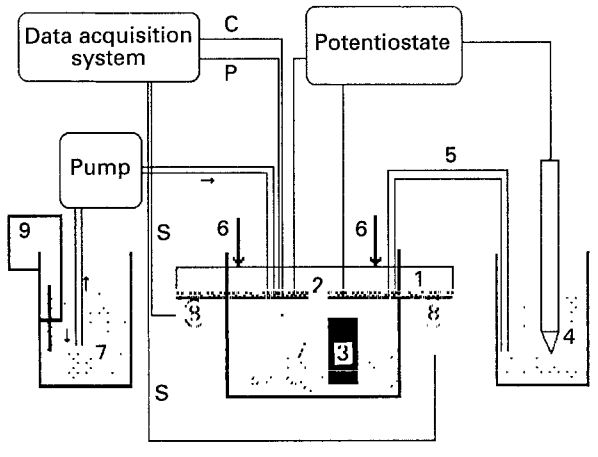

Figure 1 Experimental corrosion fatigue set-up: 1 – metal substrate; 2 – HAp coating; 1 + 2 – working electrode; 3 – counter electrode; 4 – reference electrode cell; 5 – salt bridge; 6 – loading points; 7 – simulated physiological solution; 8 – load transducers; 9 – immersion thermostatic circulator; C – corrosion current density signal; P – corrosion potential signal; S – stress signal.

2.3. Complementary testing techniques

Sample degradation was characterized morphologically using scanning electron microscopy (SEM) in a Jeol JSM 35C. Coating thickness was estimated, before and after the experiment, using optical microscopy and SEM. Energy dispersion spectroscopy (EDS), in a Noran Instruments device, was used to look for variations in the Ca/P ratio. A semi-quantitative procedure was used for computing results. For further electrochemical characterization, a.c. electrochemical impedance spectroscopy was selected, this being a very sensitive technique well-suited to coated systems [18]. Bode–Nyquist impedance spectroscopy was used and charge transfer resistance (R_{ct}) and double layer capacity (C_i) were calculated. This was done before and after corrosion fatigue testing. Five different d.c. potentials were applied: − 500, − 100, 0, 100 and 500 mV. Imposed a.c. sinusoidal wave was 10 mV, and frequency was scanned from 100 kHz to 0.005 Hz. Potentials that lay on the passive region of a potentiodynamic anodic polarization curve were selected. Two symmetrical potentials in the cathodic region were also selected. It was the intention to study potentials that will keep samples in the passive state, as expected in normal conditions in the human body, and correlate results with those obtained in the main experiments, i.e. the open-circuit corrosion fatigue tests. These tests were aimed at obtaining some kinetic information about the tested system in similar conditions to those used in the corrosion fatigue experiments. The first intention was to look for possible detachments of the coating that might have been induced by imposed potentials, and study in those conditions the substrate electrochemical behaviour. Ten points were acquired for each logarithimic decade to define the impedance spectra. This was done using a potentiostat and a frequency response analyser (FRA). Only samples tested at σ_{max} = 80 MPa (for time = 0) have undergone this test and all the tests were carried out in a ISS solution at room temperature. In-house developed software, IMPFRA®, was used to control testing parameters, acquisition steps and compute results. The value for the charge transfer resistance (R_{ct}) was calculated by adjusting a semicircle to the experimental points of the Nyquist plot (three points lying for certain in the semicircle region are selected to define the curve) and intercepting it with the $Z'(XX)$ axes. Then the value for the solution resistance (R_Ω) was deducted and the R_{ct} value obtained. To compute the value for the double layer capacity (C_i) a linear regression was applied to the experimental points lying in the linear part of the Bode plots. Then C_i was calculated assuming that $C_i = 1/IZI(f \rightarrow 0)$. This means that we have calculated the interception of the

linear regression with the log $IZI(YY)$ axes using IZI obtained in the expression referred to above.

3. Results and discussion

Corrosion fatigue results established that there was no tendency for local activation in the metal substrate, even for the 80 MPa initial stress levels. For tests carried out in HBSS solution, initially open-circuit potential was slightly decreased and then stabilized. In contrast, in ISS solution behaviour was much more unstable and after 10^6 cycles no rest potential was achieved. However, it was decided to consider the final potential (after 10^6 cycles) as the corrosion potential (E_{corr}) for the testing period. E_{corr} values were -120 mV for HBSS solution and -90 mV for ISS, as plotted in Fig. 2 and Fig. 3. The $E = f(t)$ curves were almost coincident for 80 MPa and 40 MPa, and as a consequence only the higher stress level curves are presented. Mechanical degradation levels were not significantly increased by the presence of the simulated body fluids as compared to the results obtained in air (Fig. 4). No trace of an increase in tendency to corrode was detected in open-circuit fatigue-corrosion testing. It seems that coating cracking did not change metal substrate passive state or at least did not increase its corrosion susceptibility, for the conditions used.

Coating integrity (Table I) was strongly affected by cyclic loading, reducing its thickness. Fig. 5 presents

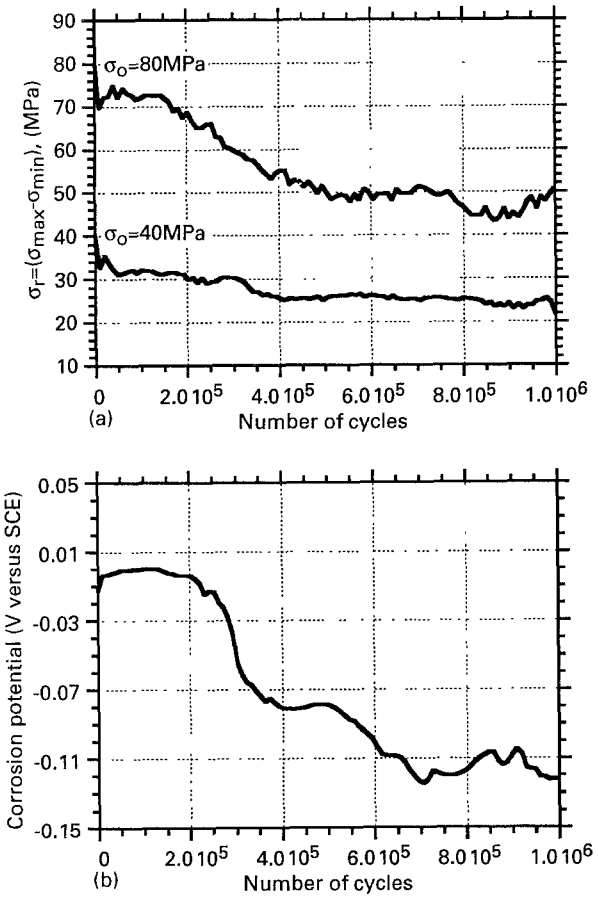

Figure 2 Corrosion fatigue results obtained in HBSS solution. Stress (a) and corrosion potential (b) were monitored simultaneously as a function of the number of cycles.

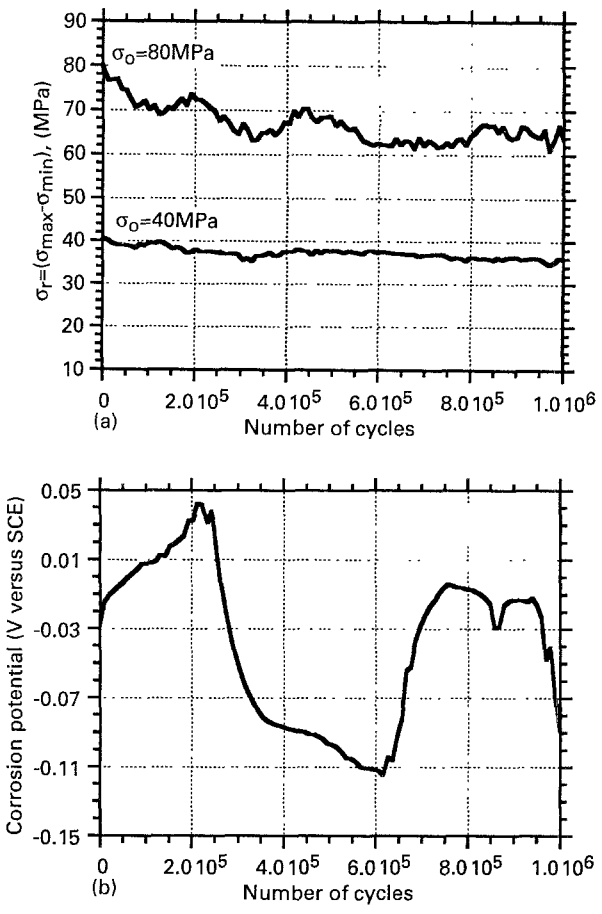

Figure 3 Corrosion fatigue results obtained in ISS Stress and corrosion potential were monitored simultaneously as a function of the number of cycles

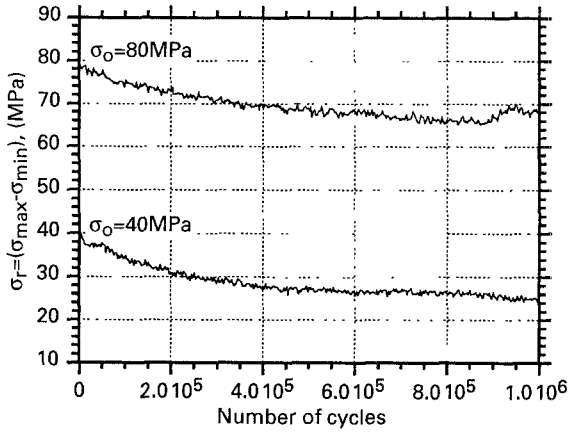

Figure 4 Fatigue results obtained in air (dry test). Stress was acquired as a function of the number of cycles.

an example of a degraded surface. An "as-received" surface is presented in Fig. 6 allowing for easier correlation. HBSS solution provoked a greater mechanical degradation of HA coatings. No significant variation in Ca/P ratio was found by EDS analysis (see Table I) after fatigue experiments, but in the case of HBSS, values tend to the equilibrium ratio for HA (1.67), while 1.70 was obtained after spraying. Cyclic loading associated with chemical attack was disadvantageous to the coating integrity. ISS solution was responsible not only for mechanical degradation but

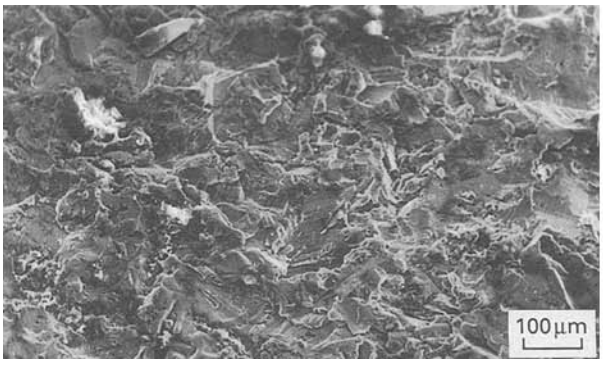

Figure 5 An example of a degraded surface. Sample tested in HBSS for 24 h

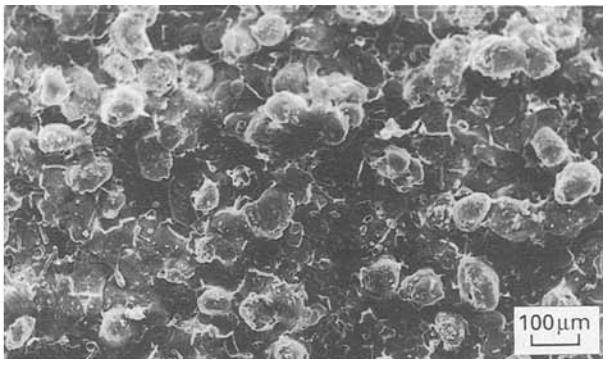

Figure 6 An "as-received" coated sample surface.

TABLE I Coating thickness, solution pH and Ca/P ratio before and after fatigue testing, in HBSS and ISS, with two different initially imposed stress levels

	Coating thickness (μm)	Initial pH	Final pH	Ca/P ratio
Control samples (non-tested)	50 ± 10	–	–	1.70
Tested in HBSS $\sigma_0 = 40$ MPa	35 ± 12	7.433 ± 0.002	6.679 ± 0.002	1.67
Tested in HBSS $\sigma_0 = 80$ MPa	28 ± 11	7.433 ± 0.002	6.649 ± 0.002	1.67
Tested in ISS $\sigma_0 = 40$ MPa	38 ± 13	6.300 ± 0.002	7.701 ± 0.002	1.70
Tested in ISS $\sigma_0 = 80$ MPa	32 ± 14	6.300 ± 0.002	7.896 ± 0.002	1.71

also for coating dissolution as may be confirmed by the calcium-released levels presented in Table II.

Table I also presents pH results. pH of HBSS solution tended to decrease after testing as opposed to that of ISS solution. These pH variations must be related to different levels of Ca, P and metal (Ti, Al, V) ions released in the two solutions. Impedance spectra were drawn to obtain information on kinetics without disturbing the sample surface state (after fatigue-corrosion testing). This technique may be used for rapid corrosion screening in poorly defined systems. Figs 7 and 8 show, respectively, Nyquist plots for a control sample and a sample tested for corrosion-fatigue in HBSS. As may be seen in the Nyquist plots, the system, presents a pseudocapacitance. This behaviour is displayed only for the lower frequencies and may be associated with an analogue circuit in which R and C_1 (in parallel) are in series with another capacitance (C_2). This second capacitance represents the adsorption of species on the porous electrode, which is responsible for the Bode plot slopes (all laying between -0.5 and -1). Due to coating porosity the influence of the adsorbed species over the electrode behaviour is well marked, particularly, as expected, in the lower frequency range. After corrosion-fatigue testing the coating is smoother and thinner and as a consequence the influence of the pseudocapacitance decreases (Bode slope increases).

The semicircles of the Nyquist plots were depressed when the applied potential diverged from the open-circuit potential. A much clear depression was found for the more anodic potential (-500 mV). If one compares the curves of Fig. 7 and Fig. 8 it is clear that after corrosion-fatigue tests the samples present a similar behaviour but a large depression of the semicircle (note scales) was detected after testing, which indicates a smaller resistance to charge transfer.

Ti-alloy substrate corrosion was ruled by charge transfer, with the Bode plot tending to -1 (Fig. 9), however, for the lower frequency range a typical Randles II response with a Warburg impedance was detected. Results (derived parameters) are not presented

TABLE II Atomic absorption spectroscopy results on Ti, Al, V and Ca amounts before and after cyclic testing at different imposed stress levels for the HBSS and ISS solutions

	Ti (ppm)	Al (ppm)	V (ppm)	Ca (ppm)
HBSS solution (control)	< 5	< 5	< 1	73
HBSS after test $\sigma_0 = 40$ MPa	< 5	< 5	< 1	76
HBSS after test $\sigma_0 = 80$ MPa	< 5	< 5	< 1	78
ISS solution (control)	< 5	< 5	< 1	430
ISS after test $\sigma_0 = 40$ MPa	< 5	< 5	< 1	1150
ISS after test $\sigma_0 = 80$ MPa	< 5	< 5	< 1	1200

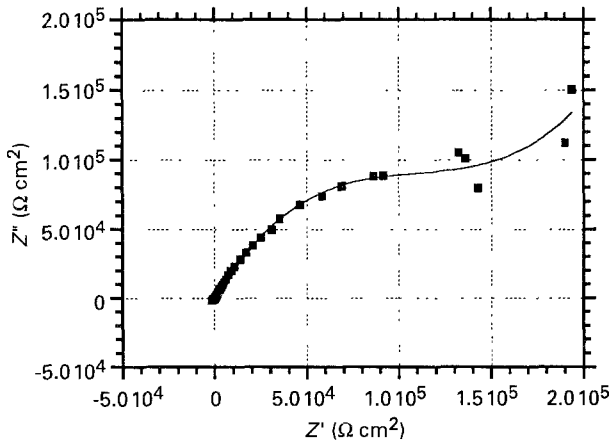

Figure 7 Nyquist plot for a control coated sample A d.c. potential of − 500 mV was applied.

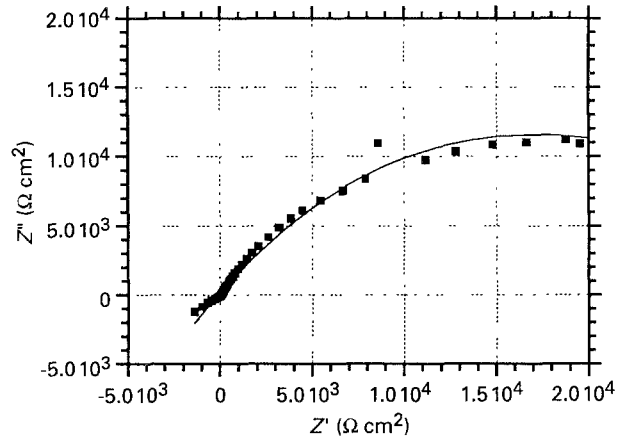

Figure 8 Nyquist plot for a sample tested for corrosion-fatigue in HBSS. A clear depression in the semicircle was detected. A d.c. potential of − 500 mV was applied

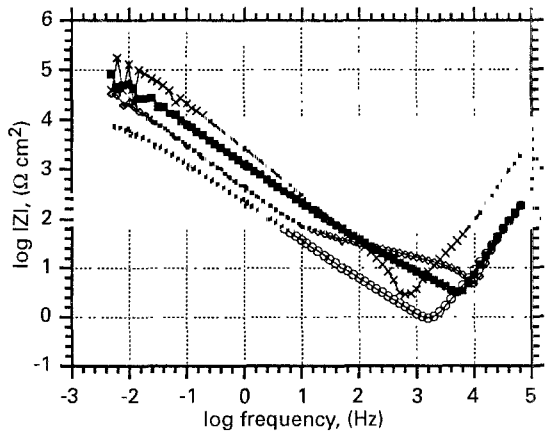

Figure 9 Bode plot for: (–■–) control sample; (–○–) sample tested for corrosion-fatigue in HBSS: (–◇–) sample tested for corrosion-fatigue in ISS; (∗) Ti–6Al–4V substrate sample. A d.c. potential of − 100 mV was applied.

because, since the porosity of the coated and uncoated systems differ significantly, they are not comparable.

A solution resistance around 60 kΩ cm^2 was found in almost every test. R_{ct} and C_i results (Table III) indicated a tendency for an increase in the corrosion kinetics after fatigue-corrosion testing. R_{ct} values were always smaller after fatigue-corrosion testing than prior to testing, for all imposed potentials. The charge transfer resistance was drastically decreased on samples which were tested for corrosion fatigue in HBSS. The lowest values for R_{ct} were obtained for the more anodic potential, − 500 mV, as expected. C_i results tended to confirm these results as C_i values were consistently higher after cyclic testing. Again HBSS was the more detrimental to coating stability. After fatigue testing Bode plot slopes (Table III) were always higher, particularly in the samples which were tested in ISS solution, indicating that sample behaviour tends to become charge transfer controlled, instead of being ruled by oxygen diffusion in the cathodic areas. This clearly indicates that, although not detected by atomic absorption spectroscopy (AAS) results presented in Table II, the samples have shown, for most of the applied d.c. potentials, higher corrosion rates after testing. It must also be stressed that

TABLE III Bode–Nyquist impedance results for samples tested in HBSS and ISS and control samples (before any testing)

Sample reference	Applied d.c. potential (mV)	Charge transfer R_{ct} resistance (kΩ cm^2)	Double layer capacity, C_i (μ F cm^{-2})	Bode plot slopes
	− 500	218	238	− 0.711
Control	− 100	617	159	− 0.708
	0	512	136	− 0.729
	100	575	175	− 0.747
	500	623	175	− 0.750
	− 500	19	1386	− 0.721
Tested in HBBS	− 100	107	936	− 0.758
	0	132	777	− 0.755
	100	107	1019	− 0.757
	500	27	1010	− 0.758
	− 500	207	379	− 0 827
Tested in ISS	− 100	507	316	− 0.819
	0	434	303	− 0.839
	100	407	338	− 0.820
	500	427	299	− 0.871

during test in HBSS some kind of hydrogel containing Ti, Al and V, together with elements of the saline solution, seemed to be formed. X-ray diffraction studies are in progress to identify this solid product. These results must be confirmed with extended testing and with potentiostatic corrosion fatigue results. Table II shows that there was no real meaning in the metal ion release levels. On the other hand, the coating, as confirmed by SEM micrographs, has shown degradation. This degradation was not only mechanical (loosening of solid particles from the substrate) but also chemical, as there seems to be a dissolution of calcium which is much more clear in ISS solution.

4. Conclusions

Hydroxylapatite coatings are not stable under the synergetic action of cyclic loading and chemical attack by simulated body fluids. Coating degradation is not only due to loosening of solid particles but also to coating dissolution. Metal substrate ion released levels appear to be insignificant and no surface activation was detected in corrosion-fatigue testing. However, Bode–Nyquist impedance results clearly show that after corrosion fatigue testing, samples corrode at higher rates. HBSS, the more complex solution, was the most aggressive to coating stability.

Acknowledgements

The support of the BRITE/EURAM Programme under project BREU-0172-C is gratefully acknowledged. The authors are also indebted to CEMUP and Dr Carlos Sa for support in SEM/EDS studies.

References

1. K SOBALLE, E. S. HANSEN, H. B. RASMUSSEN, P. H. JORGENSEN and C. BUNGER, *J. Orthop. Res.* **10** (1992) 285.
2. S. D BROWN, *Thin Solid Films* **119** (1984) 127.
3. D. P. RIVERO, J. FOX, A. K SKIPOR, R. M. URBAN and J. O. GALANTE, *J. Biomed. Mater. Res.* **22** (1988) 191.
4. M. Y. SHAREEF, P. F. MESSER and VAN R. NOORT, *Biomaterials* **14** (1993) 69.
5. R. Y WHITEHEAD, L. C. LUCAS and W. R LACEFIELD, *Clin. Mater.* **12** (1993) 31.
6. H. JI and P. M. MARQUIS, *Biomaterials* **14** (1993) 64.
7. C A. VAN BLITTERSWIJK, J. J. GROTE, W. KUYPERS, C J G. BLOK-VAN HOEK and W Th. DAEMS, *ibid.* **6** (1985) 243.
8. F. KUMMER and W. JAFFE, *J. Appl. Biomater.* **3** (1992) 211.
9. H. S. DOBBS and J L. M. ROBERTSON, in "Titanium alloys in surgical implants", ASTM STP 796, edited by H. A. Luckey and F. Kubli Jr (ASTM, 1983) p. 277.
10. M A. IMAN, A C FRAKER and C. M. GILMORE, in "Corrosion and degradation of implant materials", ASTM STP 684, edited by B. C. Syrett and A. Acharya (ASTM, 1979) p. 173.
11. L. E. SLOTER and H. R. PIEHLER, in "Corrosion and degradation of implant materials", ASTM STP 684, edited by B. C. Syrett and A. Acharya (ASTM, 1979) p. 195.
12. M MORITA, T SASADA, H HAYASHI and Y. TSUKAMOTO, *J. Biomed. Mater. Res.* **22** (1988) 529.
13. H. LIN, H. CU and K. dE GROOT, in Transactions of Fourth Biomaterials Congress, Berlin, April 1992, edited by U. Gross, p. 193.
14. S. D COOK, N. THONGPREDA, R. C. ANDERSON and R. J HADDAD Jr, *J. Biomed. Mater. Res.* **22** (1988) 287.
15. R. L REIS, F J MONTEIRO and A. GARRIDO, in "Bioceramics 5", Kyoto, November 1992, edited by T. Yamamuro, T. Kokubu and T. Nakamura (Kobunshi Kankokai, Tokyo, 1992) p. 259.
16. R A SILVA, M. A BARBOSA, O CONDE, M. C. BELO and I SUTHERLAND, *Clin. Mater.* **7** (1991) 31.
17. M A. BARBOSA, in "Bioceramics 4", London, September 1991, edited by W. Bonfield, F. W. Hastings and K E. Janmer (Butterworth-Heinemann, London, 1991) p. 325.
18. D C. SILVERMAN, *Corrosion* **46** (1990) 589.